In situ Investigation of Carboxylate Adsorption at the Fluorite/Water Interface by Sum Frequency Spectroscopy

Simon Schrödle, Fred G. Moore, and Geraldine L. Richmond*

Department of Chemistry, University of Oregon, Eugene, Oregon 97403-1253

Received: February 13, 2007; In Final Form: April 5, 2007

This work presents a study of carboxylate adsorption at the fluorite/water interface by vibrational sum frequency spectroscopy. A homologous series of monocarboxylic ions including formate, acetate, propionate, hexanoate, and dodecanoate was studied in frequency regions corresponding to the νCH and νCO/δCH response. Previously reported vibrational and Raman modes were investigated for their sum frequency activity. For a more reliable band assignment, sum frequency measurements on systematically deuterated compounds were completed and compared with calculated band positions and intensities. Different polarization configurations were utilized, together with symmetry properties of bands derived from a normal-mode analysis, to classify the observed fundamentals and overtones. Differences in chain length led to striking changes in the spectral signatures of the compounds studied and were related to the molecular structure of the adsorbates and interfacial water molecules.

1. Introduction

Adsorption processes at liquid/solid interfaces play an important role in geochemical processes and a variety of technological applications.[1−3] Here, the interaction of mineral surfaces with low molecular weight carboxylates, which are ubiquitous in soils[4,5] and large-scale industrial production, is of particular interest. Carboxylate ions can govern dissolution processes, regulate the biological availability of nutrients, and are a determining factor for the environmental transport cycle of various metals,[4] including the bioretention of chromium and other toxic pollutants. In industry, the adsorption of carboxylate ions onto particles is a common mechanism for growth inhibition and impurity inclusion during product crystallization (e.g., in the Bayer process,[6] a key step in the production of aluminum). Carboxylates have also found a variety of applications from surface modifying agents to the size-controlled synthesis of nanoparticles[7] and can act as an intermediate layer for the interaction of surfaces with other organic materials,[8] which is crucial for promising innovations like dye-sensitized solar cells.[9]

Naturally, carboxylate interactions with solid substrates have been studied by a variety of techniques with IR and Raman spectroscopy being most common for in situ investigations. While such studies are certainly useful and can reveal a fair amount of detail, they are not surface specific on a molecular scale. Even specialized methods (Fourier transform infrared−internal reflection spectroscopy, diffuse reflectance Fourier transform spectroscopy) are usually limited to substrates with rather high surface areas such as finely divided powders, suspensions, or colloids[10−12] and often require a difficult spectral separation of the adsorbate contributions from bulk background signals.

More recently, vibrational sum frequency spectroscopy (VSFS) has been employed to develop a molecular picture of adsorption processes at the solid/liquid interface. On the basis of an inherently surface specific nonlinear optical process, the coherent nature of the sum frequency generation can reveal more detailed information compared to linear techniques, especially when coupled with polarization-resolved measurements. Until now, most studies were limited to the frequency regions of νCH and νOH bands, as suitable laser sources were more readily available in the corresponding wavelength region (2800−4000 cm^{-1}). For carboxylates, the relevant bands (νC−O, νC═O) are located at larger wavelengths, typically on the order of 1300−1700 cm^{-1}, and technological advances only recently opened up this spectral region for VSFS studies.[13]

In IR and Raman investigations of carboxylates, both in solutions and adsorbed on substrates, the signature of the carboxylate group is often obscured by other bands, namely, C−H bending modes.[14] Furthermore, efforts at performing simplified group moment analysis of the experimentally resolved bands, along with the presence of overtones and the often low-resolution spectra have caused considerable disagreement and ambiguity in mode assignments.[15,16] With the additional information revealed by VSFS, combined with an ab inito calculation approach and the investigation of systematically deuterated compounds, we can resolve many of these problems.

The solid/liquid interface selected for this study, the fluorite-(CaF_2)/water interface, serves as a model system for a variety of ionic crystalline solids. Fluorite is characterized by a positive surface charge in many natural environments, especially at slightly acidic pH.[17] The sum frequency response of the neat fluorite/water interface has already been investigated,[17] and these results, together with the favorable optical properties of CaF_2 (transparent from ∼120 to 7800 nm), facilitate the experiment and the interpretation of VSFS data in related systems.

The investigation of the principal spectral features of carboxylate head groups and the clarification of peak assignments are prerequisite for any orientational analysis and also are relevant for adsorption studies with other molecules of interest (e.g., amino acids and similar biological molecules). Additionally, the frequency coverage of this study, which includes the water region of the VSF spectrum, provides a more detailed picture of the adsorption processes and the water structure near

* Author to whom correspondence should be addressed. E-mail: richmond@uoregon.edu. Fax: 541-346-5859.

10.1021/jp071248e CCC: $37.00
Published on Web 05/16/2007

the adsorbates, which is of fundamental importance for further VSFS studies in this field.

2. Background

2.1. VSFS. VSFS is a technique particularly suited for the study of interfaces. It exploits the symmetry breaking at the boundary of two isotropic media, which gives rise to a nonlinear susceptibility $\chi^{(2)}$. As these effects have been extensively treated in the literature,[18,19] only an overview of the essential concepts is given here.

For the experiment, two short laser pulses, one with fixed frequency ω_{vis} in the visible and the other tunable in the IR range (ω_{IR}), are spatially and temporally overlapped at the interface. The local fields $E(\omega_{IR})$ and $E(\omega_{vis})$ are then coupled by $\chi^{(2)}$ (eq 1) and induce a nonlinear polarization at the sum frequency $\omega_{SF} = \omega_{IR} + \omega_{vis}$

$$P_{SF}(\omega_{SF}) = \chi^{(2)}{:}E(\omega_{vis})E(\omega_{IR}) \quad (1)$$

Generally, the wavelength of the visible beam is chosen to be off resonance, thus $\chi^{(2)}$ only depends on the IR frequency, and measured sum frequency spectra are of the form

$$I_{SF}(\omega_{IR}) \propto |P_{SF}|^2 \propto |\chi^{(2)}|^2 I_{vis} I_{IR} L_{SFG}{}^2 L_{vis}{}^2 L_{IR}{}^2 \quad (2)$$

Here I_{vis} and I_{IR} denote the intensities of the incident beams, and the L terms are the Fresnel factors. Note that for a small frequency band, the Fresnel factors can be considered constant.

Phenomenologically, $\chi^{(2)}$ is treated as a coherent superposition of a nonresonant part $\chi^{(2)}_{NR}$ and resonant components of the susceptibility, $\chi^{(2)}_{R,i}$ (eq 3).

$$\chi^{(2)} = \chi^{(2)}_{NR} + \sum_i \chi^{(2)}_{R,i} \quad (3)$$

While $\chi^{(2)}_{NR}$ is assumed to be real for the CaF_2/water interface like for most common dielectric surfaces,[20] $\chi^{(2)}_{R,i}$ is complex and related to the orientationally averaged hyperpolarizabilities $<\beta^{(2)}>$ of the interfacial molecules. From $<\beta^{(2)}>$, the average orientation of adsorbates can be derived, when the molecular hyperpolarizabilities are known in the molecular frame.[21]

Given that the interface layer is isotropic (i.e., it has $C_{\infty v}$ symmetry), only 7 of the 27 tensor elements of $\chi^{(2)}$ are nonzero and of these only 4 are unique. With the lab coordinates chosen so that z lies along the interface normal and the xz-plane is the plane of incidence, they are $\chi^{(2)}_{xxz} = \chi^{(2)}_{yyz}$, $\chi^{(2)}_{xzx} = \chi^{(2)}_{yzy}$, $\chi^{(2)}_{zxx} = \chi^{(2)}_{zyy}$ and $\chi^{(2)}_{zzz}$. In addition, for ω_{vis} far from resonance, $\chi^{(2)}_{xzx} = \chi^{(2)}_{yzy} = \chi^{(2)}_{zxx} = \chi^{(2)}_{zyy}$. These four elements can be probed using combinations of incident and outgoing linearly polarized light, namely: *ssp*, *sps* (or *pss*), and *ppp*, where the letters represent light polarized parallel to the plane of incidence (*p*) or perpendicular to the plane of incidence (*s*). All polarization notations are given in the order sum frequency, visible, IR.

2.2. Fitting Procedures. VSF spectra, normalized by the intensities of the incident beams and the nonresonant response of a highly polished gold surface (to account for variations in pulse duration and beam overlap), were deconvoluted by a method developed earlier in our laboratory.[22] The line shape of the i^{th} resonance was modeled by an expression

$$\chi^{(2)}_{R,i} = A_i e^{i\gamma_i} \int_0^\infty \frac{1}{\omega_{IR} - \omega_L + i\Gamma_L} \exp\left[-\frac{(\omega_L - \omega_i)^2}{\Gamma_i^2}\right] d\omega_L \quad (4)$$

that accounts for homogeneous line broadening Γ_L (Lorentzian width, fixed at 5 cm^{-1}) and inhomogeneous broadening, Γ_i (Gaussian width). The Gaussian width combines the effect of the multitude of environments experienced by the adsorbate and the IR beam bandwidth, while the Lorentzian profile describes the inherent line width of the transition.

For overlapping bands, the phase relationship of the responses, γ_i has to be considered. For all bands observed here, phases of either 0 or π were used, as variable phases $-\pi < \gamma_\nu \leq \pi$ did not significantly improve the quality of the fits.

The effective sum frequency transition strength of a band A_i depends on the product of the number of adsorbed molecules, the orientational average of the electric transition dipole moment, and the Raman polarizability of the underlaying mode. Modes are therefore only sum frequency active if they are both Raman and IR active. Additionally, the adsorbed molecules must show a net orientation with respect to the interface.

2.3. Electronic Structure Calculations. All electronic structure modeling and normal-mode analysis have been performed using the Gaussian03 program[23] with the 6-311+g(d,p) basis set used throughout. For every carboxylate ion studied, a geometry optimization was performed followed by a normal-mode analysis and frequency calculation using the RHF and RB3LYP methods. Systematic errors in calculated frequencies were accounted for by scale factors. Values of 0.893 and 0.961 were chosen for the RHF and RB3LYP calculations,[24] respectively.

3. Experimental Methods

3.1. Vibrational Sum Frequency Spectrometer. The experimental instrumentation is based on a commercially available VSF spectrometer (Ekspla, Vilnius, Lithuania). The visible (532 nm) and IR (1000−4300 cm^{-1}, bandwidth <6 cm^{-1}) beams (30 ps pulse duration, 10 Hz repetition rate) reach the solid/liquid interface in a copropagating configuration. A CaF_2 prism (68°) was used and the beam geometry adjusted to near-critical incidence (17° IR, 20.5° vis). It has been noted before that this total internal reflection geometry greatly enhances the sum frequency (SF) signal.[25] For detection, residual vis and IR energy was blocked by a high-efficiency notch filter, and the SF signal was detected by a photomultiplier tube (PMT) attached to a monochromator.

Prior to each measurement, the prism surface was equilibrated with the sample until a stable sum-frequency response was reached, except for experiments at partial coverage.

Spectra were usually recorded at 1 cm^{-1} resolution in the 1400/2800−3000 cm^{-1} region and at 4 cm^{-1} for higher wavenumbers. The actual intensities of the IR and vis beams (typically 300 and 100 μJ, respectively) were recorded during acquisition, and raw data were normalized for the fluctuations in beam power as well as the dark current of the PMT. The resulting spectra were calibrated against the nonresonant SF response of a thin gold layer measured under similar conditions to correct for frequency dependent variations of the SF generation efficiency. The alignment of the spectrometer was frequently checked against neat water.

Around 1410 and 1525 cm^{-1}, a small resonant background was observed, which did not seem to arise from the solid/liquid interface but rather from the prism sides exposed to air. Carboxylate spectra were thus corrected for any water background signal.

3.2. Materials. All salts used were at least of analytical purity and obtained from commercial sources. The deuterated materials were purchased from CDN Isotopes (Quebec, Canada) or Cambridge Isotope Laboratories (Andover, MA) and had a high

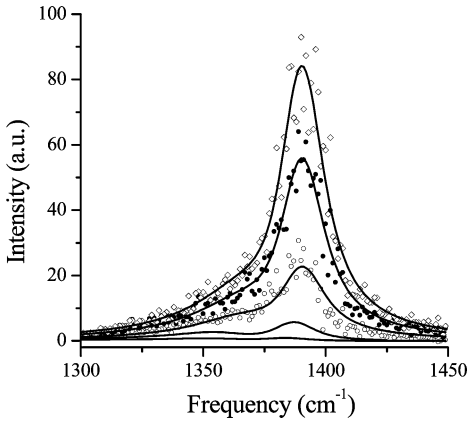

Figure 1. VSF spectra (*ssp*) of the sodium formate (aq)/CaF_2 interface as a function of formate concentration (from bottom to top): 15.3, 46.0, 182, 333, 462 mM. Some data (15.3, 46.0 mM) omitted for clarity. Curve fits shown as solid lines.

degree of enrichment (>98%). Solutions were prepared volumetrically with the pH controlled (5.5−6) by the addition of NaOH solution (pH meter, calibrated glass electrode) or trace amounts of hydrochloric acid.

All water used for the preparation of solutions and rinsing of glassware was purified by a Barnstead NANOpure II system (resistivity > 18 MΩcm).

The fluorite prism was regularly cleaned by soaking in 0.1 mol/L hydrochloric acid and subsequent polishing with 0.05 micron Al_2O_3 powder to avoid any buildup of carbonation layers[26,27] and to remove other impurities. At intervals, the prism was more extensively cleaned by soaking in concentrated sulfuric acid with added ammonium peroxodisulfate as an oxidizer to remove any trace organic contaminants, followed by soaking in 0.1 mol/L hydrochloric acid and methanol (HPLC grade).

4. Results and Discussion

4.1. Formate. Surface speciation of formate is of importance for many catalytic processes used in industry, and some VSFS studies have been reported but were limited to ultrahigh vacuum (UHV) conditions and Ni[28−30] or MgO[31,32] substrates. These investigations mainly focused on the 2700 to 3100 cm^{-1} spectral region where two bands were observed, located at ∼2860 and ∼2950 cm^{-1}.[28,29,31] Some investigators ascribe these bands to different formate species[29,32] or observe only one band (at 2948 cm^{-1}) and assign it to the νCH symmetric stretch,[28] while claiming that combination bands known from IR studies would not be detectable in the VSF spectra due to their presumably vanishing Raman moment.[28] On MgO(001), only a single band at 2870 cm^{-1} was reported[31] and assigned to the νCH symmetric stretch. Using (linear) infrared reflection−adsorption spectroscopy (IRRAS), the same investigators observe peaks at 2854 cm^{-1} (δCH + ν_{as}CO) and 2943 cm^{-1} (νCH),[33] arguing that the stronger band (2943 cm^{-1}) should be the fundamental.

These findings are at odds with reports (IRRAS) by others,[34,35] which provide data of higher resolution and spectral coverage. These latter reports document three bands at 1365, 2895, and 2950 cm^{-1} on Cu(110)[34] or 1365, 2840, and 2942 cm^{-1} on Ni-(110),[35] which were assigned to the νCO symmetric stretch, the νCH symmetric stretch, and a δCH + ν_{as}CO combination mode, respectively.

From our work, Figure 1 shows the VSF spectra of formate-(aq) at the CaF_2 interface as a function of formate concentration in the 1300 to 1450 cm^{-1} wavenumber region. It clearly reveals the presence of two bands, centered around 1359 and 1386 cm^{-1} (Table 1).

To interpret these bands, one needs an appreciation of the symmetry of the system. For surface-adsorbed formate, four different symmetries can be distinguished and are characterized by the alignment of the C−H bond with respect to the surface normal (Figure 2). For perpendicular alignment ($\alpha = 0$, $\beta = 0$), the symmetry is C_{2v}, which is lowered to C_S ($\alpha \neq 0$, $\beta = 0$; $\alpha = 0$, $\beta \neq 0$)) or C_1 ($\alpha \neq 0$, $\beta \neq 0$) depending on the tilt angles α and β.

From our normal-mode analysis, two bands can be expected in the 1300 cm^{-1} region. These correspond to the A_1 and B_2 irreducible representations (C_{2v}). Note that for all symmetries with $\alpha = 0$, the B_2 mode is VSF inactive under *ssp* conditions due to its negligible dipole moment component perpendicular to the surface (equivalent to the surface selection rule of IR spectroscopy).[36]

However, the experimental peak frequencies are too closely spaced to allow for a direct assignment by comparison with calculations (Table 1) or Fourier transform IR (FT-IR) and Raman spectra, where the bands are well separated with a significantly lower amplitude of the band at 1386 cm^{-1}.[37,38] The observed results could be a single resonance split by vibrational coupling phenomena or different formate species, which were often held responsible for the appearance of multiple peaks,[29,32,35,39] and not two distinct bands.

To clarify the situation, VSFS experiments were carried out at relatively low adsorbate concentrations and deuterated formate was used, for which the δCD mode is shifted to far lower energies than the corresponding mode (Table 1) of nondeuterated formate.[40] The VSF spectra of both compounds at two different concentrations are compared in Figure 3. Because the deuteration removed the 1386 cm^{-1} band, only the VSF signal at ∼1350 cm^{-1} is caused by the νCO symmetric stretch of adsorbed formate, while the higher frequency peak can now be assigned to the δCH in-plane bending mode. The high intensity of the latter is quite surprising, as these two modes have perpendicular dipole moment vectors and thus $\alpha \neq 0$ (Figure 2). While UHV studies on metal or metal oxide-adsorbed formate often discussed perpendicular alignment in a bidentate configuration,[29,31,33] at the liquid/CaF_2 interface the alignment cannot be perpendicular in the symmetry plane. This indicates an inequality of the formate oxygen sites in the bonding geometry at ionic mineral surfaces.

In the 2800−3800 cm^{-1} range, the VSF spectra of aqueous solutions are dominated by the response of water molecules in different states of order,[17] which give rise to spectral intensity typically described by two broad bands at ∼3200 and ∼3450 cm^{-1} (∼ pH 5.5; *ssp* polarization). Spectra of our study are shown in Figure 4. A notable decrease of the water amplitudes was observed with increasing formate concentration. The intensity of the band at ∼3200 cm^{-1}, which is usually ascribed to tetrahedrally coordinated water, decreases more rapidly than that of the band at ∼3450 cm^{-1} (weaker-bonded water molecules with either asymmetric or bifurcated hydrogen bonds),[17] and two new bands appear below 3000 cm^{-1}. A careful analysis of the VSF response for the 333 mM sample using different polarization schemes (Figure 5) reveals the existence of a total of three bands, located at 2730, 2872, and 2984 cm^{-1} (Table 1). The higher two bands seem to share the same symmetry as indicated by the ratios of the *ssp* and *sps* amplitudes, respectively. As there is only one fundamental band to be expected in this region from the normal-mode analysis of formate (Table

TABLE 1: Fit Parameters of Sodium Formate and Sodium Acetate (aq) Derived from VSF Spectra at the Liquid/CaF_2 Interface (*ssp* Polarization)[a]

experimental					calculated					
c[b]	ν^c	ϕ	Γ^c	mode	$\nu_1{}^{c,d}$	$IR_1{}^e$	$RA_1{}^f$	$\nu_2{}^{c,g}$	$IR_2{}^e$	$RA_2{}^f$
				HCOONa (aq)/CaF_2						
15.3	1358	ϕ_0	19.1	ν_sCO	1323	204	14	1285	149	32
46.0	1359	ϕ_0	19.8	ν_sCO						
15.4	1385	ϕ_0	8.6	δCH	1353	45.7	5.7	1321	11.6	5.6
46.0	1387	ϕ_0	7.4	δCH						
333	2730	ϕ_1	27.2	2 ν_sCO						
333	2872	ϕ_1	32.7	νCH	2498	534	280	2468	611	400
333	2984	ϕ_1	31.5	δCH + ν_{as}CO						
				DCOONa (aq)/CaF_2						
				δCD	995	6.8	3.2	969	1.8	2.9
15.3	1352	ϕ_0	12.9	ν_sCO	1308	152	11	1273	111	22
46.0	1351	ϕ_0	7.9	ν_sCO						
				CH_3COONa (aq)/CaF_2						
19.8−333[h]	1444	ϕ_0	19.2	ν_a	1358	385	24.4	1293	337	86.5
46	1451	ϕ_0	20.3	ν_a						
19.8−333[h]	1467	ϕ_0	12.4	ν_b (δCH_3)	1412	22.1	7.1	1407	22.3	8.4
46	1464	ϕ_0	10.2	ν_b (δCH_3)						
182	2939	ϕ_1	12.2	ν_sCH	2801	43.6	145	2880	48.6	138
333	2950	ϕ_1	12.2	ν_sCH						
				CH_3COONa (D_2O)/CaF_2						
46	2949	ϕ_1	12.9	ν_sCH						
				CD_3COONa (aq)/CaF_2						
46	1440	ϕ_0	12.9	ν_sCO	1347	421	21.9	1291	330	76.9
46	1474	ϕ_0	8.1	ν_sCO + 34						

[a] Also listed are calculated frequencies, together with estimated IR and Raman activities (IR and RA, respectively), along with relative phases (ϕ) of the bands. [b] In mM. [c] In cm^{-1}. [d] RHF method. [e] In km $mole^{-1}$. [f] In $Å^4$ u^{-1}. [g] RB3LYP method. [h] Global fit.

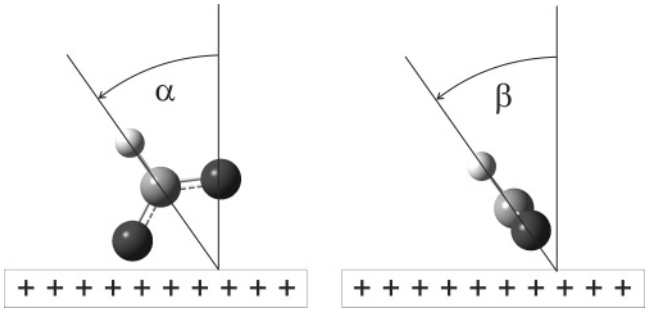

Figure 2. Tilting of the formate ion relative to the surface normal.

1; νCH at 2840[41] or 2870 cm^{-1} [37] in solid sodium formate), two of the peaks can be assigned to combination tones, 2 ν_sCO (2·1359) = 2718 cm^{-1} ≈ 2730 cm^{-1}) and δCH + ν_{as}CO. Another possible overtone δCH + ν_sCO (2745 cm^{-1}) cannot gain intensity from Fermi resonance with the νCH symmetric stretch, because it does not share the same symmetry (A_1) in contrast to δCH + ν_{as}CO ($B_2 \cdot B_2 = A_1$), which has a shared symmetry with νCH and thus fulfills the requirements for band enhancement by Fermi resonance. Note that the antisymmetric ν_{as}CO stretch itself is not Raman active[37] and could not be detected in the VSF spectrum. Its position, known from IR spectra of formate either adsorbed onto TiO_2,[38] in solution,[38] or in the solid state,[37] falls within the range of 1540−1620 cm^{-1}, corresponding to ∼2925−3005 cm^{-1} for the δCH + ν_{as}CO combination band. Keeping in mind that the separation of the component modes is usually increased by a Fermi resonance,[42] the band found at 2984 cm^{-1} in the VSF spectra can be clearly attributed to the overtone, while the fundamental (νCH) for formate at the liquid/CaF_2 interface is found at 2872 cm^{-1}. A detailed analysis of formate orientation using the intensity of the identified modes under different polarization schemes is beyond the scope of this paper and will be reported elsewhere.[43]

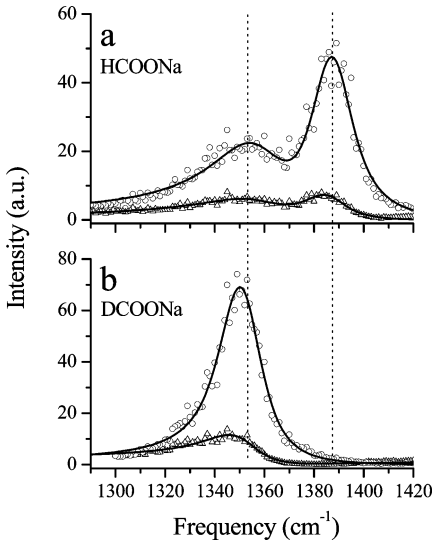

Figure 3. VSF spectra of the sodium formate (aq)/CaF_2 interface. Effect of H/D substitution on the νCO and δCH regions (triangles, 15.3 mM; circles, 46.0 mM). Curve fits shown as solid lines.

4.2. Acetate. To our knowledge, no VSFS study of acetate at solid/liquid interfaces has been reported. As with formate, the few studies of any sort[44] are limited to vacuum conditions and the 2800−3000 cm^{-1} region where a single band at ∼2950 cm^{-1} was identified. The IR spectra of the acetate ion have been subject to a number of investigations.[15,37,45,46] Only with the help of $^{13}C/^2H$ isotope substitution were disagreements in band assignments rectified (bulk measurements).[47] These disagreements arose because investigators often did not recognize the strong mixing of δCH_3 (methyl deformation) and ν_sCO modes,[48] which are both located in the 1330−1500 cm^{-1} spectral region. Consequently, there is no one normal mode confined to the carboxylate group; rather there is a strong interaction

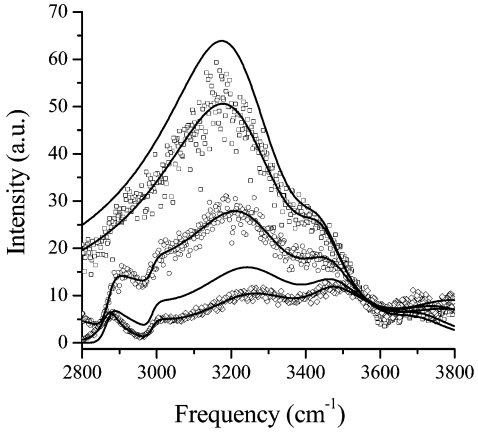

Figure 4. VSF spectra (*ssp*) of the sodium formate (aq)/CaF_2 interface as a function of formate concentration (from bottom to top): 462, 333, 182, 39.2, 0 mM. Some data (0 mM, 333 mM) omitted for clarity. Curve fits shown as solid lines.

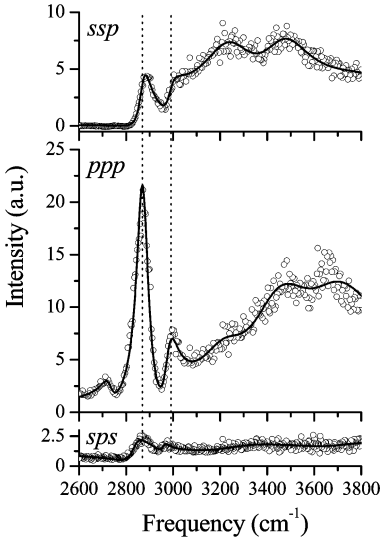

Figure 5. VSF spectra of the sodium formate (aq)/CaF_2 interface in different polarization schemes (333 mM). Curve fits shown as solid lines.

between various local motions of the molecule.[47] A potential energy distribution calculation performed by others[47] reveals the presence of two rather broad bands at ~1407 and 1423 cm^{-1}, which are attributed to a combination of $\delta_{as}CH_3$ (74%) + ν_s-CO and ν_sCO (66%) + $\delta_{as}CH_3$ (18%) + δOCO + νCC (both A′ representation of C_S) and another CH_3 deformation band (δCH_3) at ~1440 cm^{-1} (A″).

Our sum frequency spectra obtained for various concentrations of acetate(aq) at the liquid/CaF_2 interface (Figure 6) only show one band at ~1460 cm^{-1} in the frequency range under consideration as displayed in Figure 6a. While the peak is almost symmetrical at higher concentrations, significant broadening toward lower energies occurs when the concentration is decreased. Furthermore, a sum of two spectral terms was found necessary to accurately model the spectra over a larger concentration range. To get more reliable results, the whole set of concentration-dependent spectra was fit simultaneously to two bands with their Gaussian width and peak position kept constant throughout the series (Table 1, Figure 6b).

Interestingly, the values of 1444 and 1467 cm^{-1} (ν_a and ν_b in Table 1) measured here differ by 23 cm^{-1} compared to the 17 cm^{-1} separation and red shift of the two bands of solid sodium acetate (1423, 1440 cm^{-1}),[47] which are resolvable at

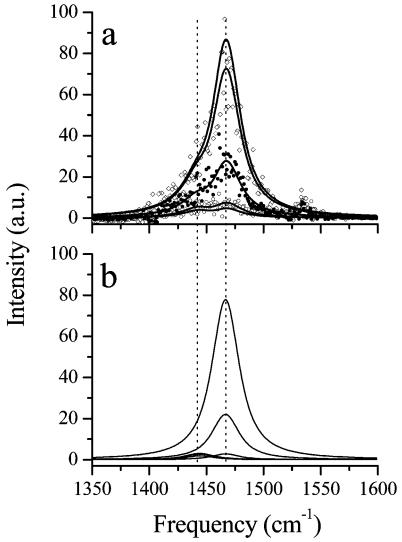

Figure 6. VSF spectra (*ssp*) of the sodium acetate (aq)/CaF_2 interface as a function of acetate concentration (from bottom to top): (a) 19.8, 39.2, 76.9, 182, 333 mM. Solid lines are fits. Decompositions of the fit spectra at selected concentrations shown as solid lines (b): 19.8, 76.9, 333 mM.

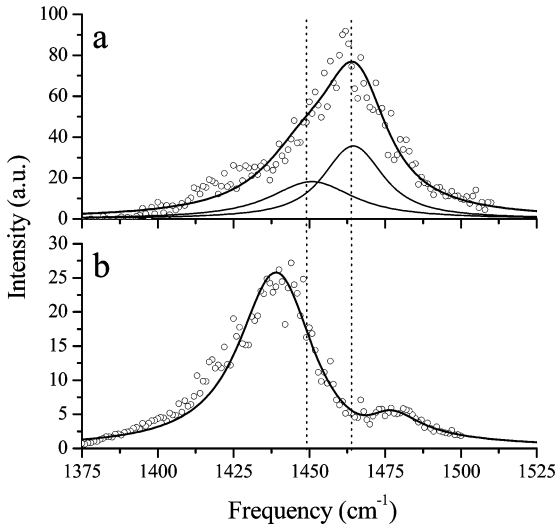

Figure 7. VSF spectra (*ssp*) of the (a) sodium acetate(aq)/CaF_2 and (b) sodium acetate-d_3/CaF_2 interface at 46 mM. Solid lines represent fits of the data. Contributing spectral peaks are shown in (a).

low temperatures (80 K). The shift toward higher energies for the CaF_2 surface follows the expected trend caused by the stronger electrostatic forces acting upon the molecule when close to a divalent ion (Ca^{2+}) as opposed to Na^+ in the salt used for the IR study.[47,48] Thus, we can initially assign the ν_a band to a ν_sCO mode, with appreciable contributions of other modes, and the 1467 cm^{-1} band (ν_b) to δCH_3. By analogy with solid sodium acetate, a third band would be expected at ~1430 cm^{-1}, which could not be identified in the VSF spectra. This is consistent with our calculations showing weaker IR and Raman intensities for this mode than for the other modes.

To further corroborate the present band assignment, experiments were performed with hydrogenated and deuterated sodium acetate at 46 mM (Figure 7). From the normal-mode analysis (Table 1) and from the potential energy distribution,[47] only one band is expected with the predominant local modes being νCO (89%, 21% νCC, and 20% δOCO). Even though the $\delta_{as}CH_3$ contribution is missing compared to the nondeuterated acetate, only a small frequency shift was observed for the mixed νCO

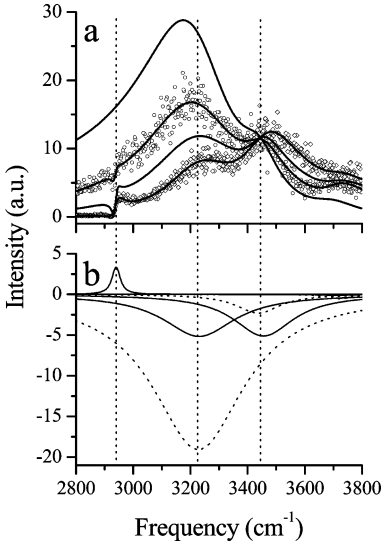

Figure 8. VSF spectra (*ssp*) of the sodium acetate (aq)/CaF_2 interface as a function of acetate concentration (a) (from bottom to top): 333, 182, 77, 0 mM). Some data (0 mM, 182 mM) omitted for clarity. Curve fits and decompositions of the fit spectra at selected concentrations shown as lines (b): 0 dotted, 333 mM solid line.

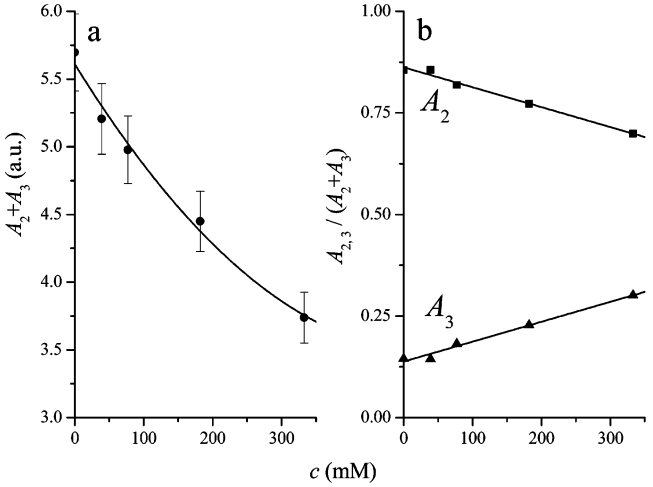

Figure 9. Water amplitudes A_2 and A_3 as a function of acetate concentration obtained from fits of the VSF spectra of sodium acetate (aq) (a) total amplitude and (b) normalized values of individual contributions. Solid lines are guides to the eye only.

mode in the IR spectra of the sodium salts.[47] Correspondingly, in the VSF spectrum of deuterated acetate, the νCO band was found at ~1440 cm^{-1}, only slightly lower than the value of ν_a in the nondeuterated compound (Figure 7a). Considering the uncertainties involved in fitting two overlapping bands, the agreement of the band positions is good and thus confirms the initial assignment. An additional low-amplitude band observed at ~1474 cm^{-1} might be due to coupling with a low-energy transition of the adsorbed acetate similar to a lattice mode. Note that the antisymmetric CO stretch (ν_{as}CO), which has a strong band in the IR spectrum at ~1555−1585 cm^{-1},[37,46,47] could not be observed in the VSF spectra, because it is virtually Raman inactive[37] and therefore not detectable by VSFS. The spurious signals visible at ~1530 cm^{-1} in some of the spectra are artifacts not associated with carboxylate adsorption.

Figure 8 shows VSF spectra in the 2800−3800 cm^{-1} region and decompositions of fit spectra at selected concentrations (Figure 8b). Only one peak from sodium acetate is observed in addition to the bands already present in neat water for all concentrations. It is located at ~2945 cm^{-1} and can be attributed to the CH_3 symmetric stretch of the adsorbed acetate (ν_sCH, Table 1), corresponding to 2936 cm^{-1} in solid sodium acetate.[37] The antisymmetric stretch (~2990 cm^{-1}[37]) could not be observed in VSF spectra. As it is expected to have a lower VSF amplitude than the symmetric mode due to its low Raman activity,[37] further experiments were performed with different polarization schemes (*ppp* and *sps*) and with sodium acetate dissolved in D_2O, to exclude obscuring of signals by the strong bands of H_2O present in this spectral region. No additional bands, however, were found. Note that the phase of the acetate ν_sCH band at 2945 cm^{-1} is shifted by π with respect to the water modes.

Figure 8b shows further details of the spectral features, including those arising from water, represented by solid and dotted lines. Apart from the bands at ~3200 and ~3450 cm^{-1} already considered for the formate(aq) solutions, a small additional band at ~3710 cm^{-1}, accounting for about ~5% of the total amplitude, was found to be necessary for a good description of the data. Its physical origin might be similar to a process (~3660 cm^{-1}) observed as a sharp peak at higher pH values[17] at the neat water/CaF_2 interface or near hydrophobic surfaces and could be associated with an OH mode of only partly hydrogen-bonded water molecules. With the focus on the main water modes characterized by amplitudes A_2 (3200 cm^{-1}) and A_3 (3450 cm^{-1}), a noticeable decrease of the total water response upon addition of acetate was found (Figure 9a). At the neat water/CaF_2 interface, preferential orientation of water molecules arises from the alignment of the water dipoles parallel to the interfacial electric field caused by a positive surface charge at the fluoride deficient CaF_2 surface.[17] When acetate is adsorbed, screening of this charge occurs, and (neutral) water dipoles have to compete with the negatively charged carboxylate ions close to the liquid/solid interface. This will first disturb the highly structured band at ~3200 cm^{-1}, attributed to tetrahedrally bonded water, and it will to a lesser extent perturb the signature of more disordered water molecules at ~3450 cm^{-1} (Figure 9b). It has been postulated that water molecules close to a liquid/solid interface can be oriented well beyond the first molecular layer,[49] and this seems to be the case here. Notably, even with a significant (333 mM) concentration of acetate present more than half of the original response remains (Figure 9a). Longer-chain carboxylates (e.g., hexanoate, decanoate, stearate[22]) are observed to disturb the water structure in both the tetrahedrally coordinated and weakly bonded states much more efficiently and at far lower concentrations.

4.3. Propionate. As the next member in the homologous series of aliphatic carboxylates, propionate incorporates a methylene group between the carboxylate headgroup and the CH_3 terminus. This molecular structure limits the flexibility of the molecule and fixes the orientation of the dipoles of these groups at an angle of ~60°. Thus, significant changes especially in the headgroup region of the VSF spectrum can be expected and are found. Over a broad concentration range (Figure 10), two prominent features were identified and are located at ~1447 and 1477 cm^{-1} (Table 2). The peak positions are almost invariant with propionate concentration in the liquid phase in equilibrium with adsorbed carboxylate at the CaF_2/liquid interface. This indicates a constant mode of adsorption up to quite high concentrations (333 mM). Conventionally, a band ~1410−1430 cm^{-1} is attributed to a νCO symmetric stretch vibration.[14,16] However, a more detailed vibrational analysis of the propionate ion in the solid state[16] revealed a number of fundamental modes within the range from 1400 to 1500 cm^{-1},

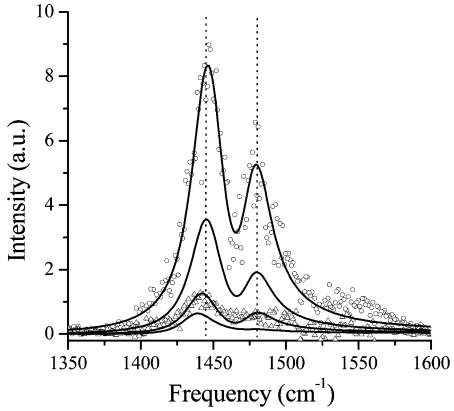

Figure 10. VSF spectra (*ssp*) of the sodium propionate (aq)/CaF_2 interface as a function of propionate concentration (from bottom to top): 8.0, 15.9, 54.5, 162 mM. Some data (8.0 mM, 54.5 mM) omitted for clarity. Solid lines are fits.

TABLE 2: Fit Parameters of Sodium Propionate (aq) Derived from VSF Spectra at the Liquid/CaF_2 Interface (*ssp* Polarization, except Where Stated Otherwise)[a]

c[b]	ν^c	ϕ	Γ^c	mode
	CH_3CH_2COONa (aq)/CaF_2			
8−162[d]	1447	ϕ_0	11.5	ν_a
333	1450	ϕ_0	8.9	ν_a
8−162[d]	1477	ϕ_0	11.1	ν_b
333	1479	ϕ_0	8.8	ν_b
333	2890	ϕ_1	18.4	ν_sCH
333	2953	ϕ_1	12.0	$2\nu_b$
333	2992	$\phi_1 + \pi$	9.3	ν_{as}CH
	CH_3CH_2COONa (D_2O)/CaF_2			
46	2891	ϕ_1	17.0	ν_sCH
46	2950	ϕ_1	11.5	$2\nu_b$
46	2990	$\phi_1 + \pi$	25.6	ν_{as}CH
46[e]	2895	ϕ_1	6.7	ν_sCH
46[e]	2955	ϕ_1	8.9	$2\nu_b$
46[e]	2993	ϕ_1	16.3	ν_{as}CH
46[f]	2987	ϕ_1	16.1	ν_{as}CH
	CD$_3$$CH_2COONa$ (aq)/CaF_2			
333	1454	ϕ_0	17.2	ν_a
333	2933	ϕ_1	29.5	ν_sCH
	CH_3CD_2COONa (aq)/CaF_2			
333	1445	ϕ_0	14.9	ν_a
333	1476	ϕ_0	10.8	ν_b
333	2894	ϕ_1	7.8	ν_sCH
333	2948	ϕ_1	7.0	$2\nu_b$
333	2979	$\phi_1 + \pi$	18.2	ν_{as}CH
	CD$_3$$CD_2COONa$ (aq)/CaF_2			
333	1449	ϕ_0	16.1	ν_a

[a] Also given are the relative phases (ϕ) of the bands. [b] In mM. [c] In cm^{-1}. [d] Global fit. [e] *ppp* polarization. [f] *sps* polarization.

corresponding to coupled vibrations of νCO, νCC, and δCH_3 modes as well as a (rather pure) methyl deformation mode. To elucidate the nature of the bands observed in the VSF spectrum, experiments with systematically deuterated compounds were carried out. Figure 11a−d shows a comparison of VSF spectra of propionate in its nondeuterated form with methyl-deuterated, methylene-deuterated, and perdeuterated propionate. Interestingly, the band at ~1477 cm^{-1} is absent for all molecules with a deuterated CH_3 group. Therefore, it can be assigned to the δCH_3 (methyl deformation) mode, located at ~1465 cm^{-1} in the IR and Raman spectra of propionate[14] in both its solid state and in aqueous solution.

The ~1447 cm^{-1} band can be observed for all deuteration patterns, however its width and position change notably. As virtually identical adsorption characteristics can be expected for

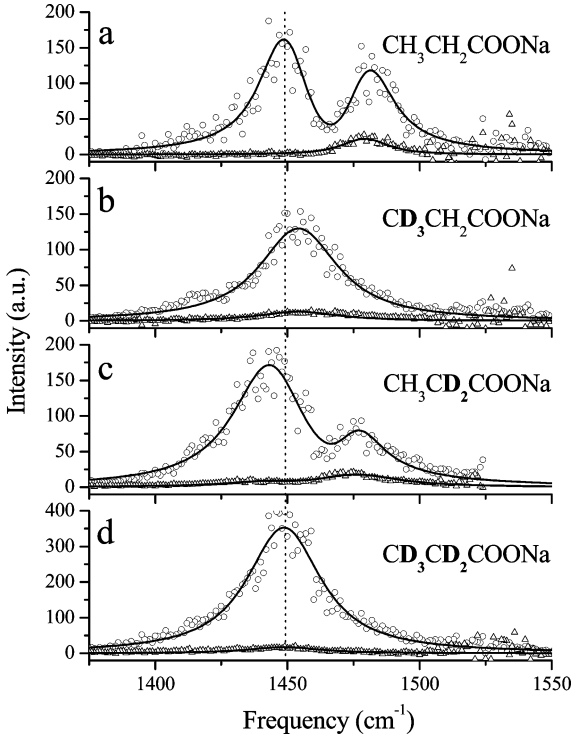

Figure 11. Comparison of VSF spectra of sodium propionate (aq) (333 mM) at the CaF_2 solid/liquid interface (a) CH_3CH_2COONa, (b) CD_3CH_2COONa, (c) CH_3CD_2COONa, and (d) CD_3CD_2COONa. Polarization schemes are *ssp* (circles) and *ppp* (triangles), respectively.

molecules only differing in their isotopic composition, these changes have to be attributed to varying coupling of the νCO motion with other group vibrations and strong coupling of the ν_sCO, especially with CH deformation modes. This is consistent with findings in IR studies of the related monosubstituted acetate ions.[48]

Usually, δCH_3 bands are rather weak in the IR spectrum,[14] but it is likely that energy transfer from the 1447 cm^{-1} mode occurs, which increases the amplitude of δCH_3. Notably, the δCH_3 amplitude is smaller for methylene-deuterated propionate (Figure 11c), because the missing contribution of the CH_2 group to the ~1445 cm^{-1} mode makes energy transfer along the chain more difficult.

The only two published VSF studies of adsorbed propionate were done on Ni/NiO surfaces under UHV conditions and are limited to the 2800−3100 cm^{-1} region.[29,50] Within this frequency range, three bands were identified at 2885, 2948, and 2990 cm^{-1}.[50] In both reports the lower two peaks were assigned to the CH_2 and CH_3 symmetric stretch, respectively. However, the assignment for the 2990 cm^{-1} band was in question and was either attributed to the CH_2[50] or CH_3[29] antisymmetric stretch.

In our work at the CaF_2/water interface, two prominent peaks were found at 2890 and 2953 cm^{-1} (Figure 12, Table 2) in addition to the broad water bands already discussed for acetate. At the highest concentration, a further band is necessary for a satisfactory fit of the experimental data and was located at 2992 cm^{-1}. A phase shift of π was found relative to the bands at 2890 and 2953 cm^{-1}. As a more detailed investigation in this frequency range is made difficult by the underling strong water response, measurements in D_2O were conducted. The resulting spectra are shown in Figure 13a. With the use of different polarization schemes (*ssp*, *ppp*, and *sps*) more information about the nature of a VSF active mode can be obtained from rather general selection rules.[51−53] In particular, symmetric stretch

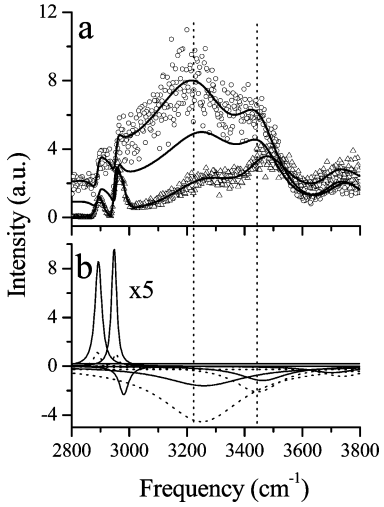

Figure 12. VSF spectra (*ssp*) of the sodium propionate (aq)/CaF_2 interface as a function of propionate concentration (a) (from bottom to top): 182, 77, 39 mM. Solid lines are fits. (b) Decompositions of the fit spectra are shown for 39 mM, dotted line, and 182 mM, solid line. Note that contributions below 3100 cm^{-1} are shown with 5 times their actual amplitude.

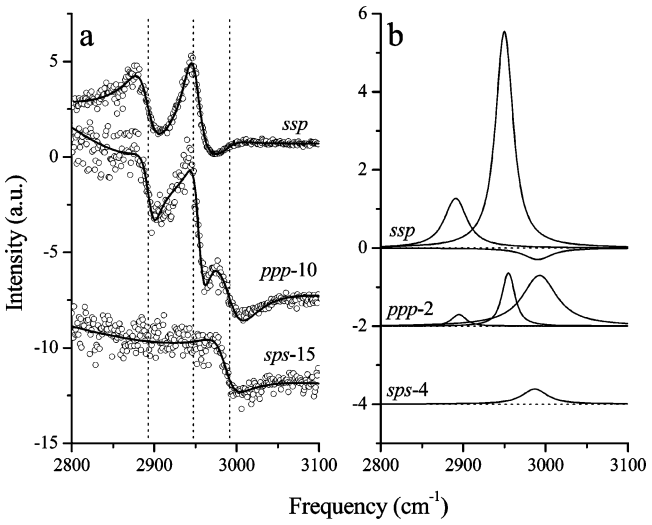

Figure 13. VSF spectra of the of the sodium propionate (D_2O)/CaF_2 interface using different polarization schemes (a) (46 mM). Decompositions of fit spectra (b) are also shown (see text). Spectra are offset for clarity by the given values.

modes of methyl and methylene groups should be virtually absent in the *sps* spectra and negatively interfere with any asymmetric stretch modes in *ssp* polarization.[52,53] Note that the phase relation between bands in the *ppp* spectrum is more variable, as several susceptibility tensor elements contribute.[25] It thus follows that the bands at ~2890 and ~2950 cm^{-1} belong to symmetric modes (Figure 13a,b, Table 2), whereas the ~2990 cm^{-1} band originates from an antisymmetric mode. Following the same methodology employed for the 1400−1500 cm^{-1} region, deuterated propionates were studied (Figure 14a−d, Table 2). All three bands were observed for both the nondeuterated propionate and CH_3CD_2COONa and can therefore be considered CH_3 bands, while the CH_2 band (symmetric stretch at 2933 cm^{-1}) is weaker and largely obscured for CH_3CH_2-COONa (Figure 14a,b). Consequently, of the 2890 and 2950 cm^{-1} bands (which share the same symmetry) one must be an overtone, enhanced by Fermi resonance, although Yuzawa et al. argue that such bands can be excluded in the case of propionate.[50] In agreement with assignments of related compounds[51] and the close match of the calculated frequency for the methyl deformation overtone ($2 \times \delta CH_3$: 2×1477 cm^{-1} = 2954 cm^{-1}; Table 2), the peak at ~2890 cm^{-1} represents the fundamental.

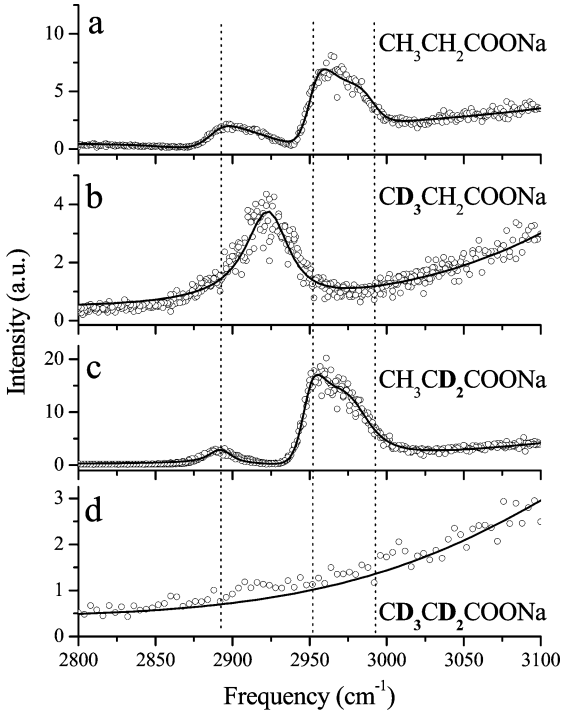

Figure 14. Comparison of VSF spectra of deuterated sodium propionate (aq) (333 mM) at the CaF_2 solid/liquid interface (a) CH_3CH_2-COONa, (b) CD_3CH_2COONa, (c) CH_3CD_2COONa, and (d) CD_3CD_2-COONa. All spectra (circles) were recorded using the *ssp* polarization scheme. Solid lines are fits.

4.4. Higher Carboxylates. In situ VSF spectroscopic measurements in the 2800−3800 cm^{-1} region for a series of long-chain carboxylates, namely hexanoate, decanoate, and stearate, have been reported before.[22] It was shown that the chain length has a strong effect on the adsorption onto CaF_2 surfaces from aqueous solutions. Long-chain ions were found to adsorb at far lower concentrations (in the micromolar regime) and form hydrophobic monolayers of sufficient thickness and coverage to suppress almost totally the response of interfacial water.[22] These results were reproduced for this study and provide insights into the orientation of the CH_3 terminus and water structure. Additionally, we report here the first results in the spectral region of the headgroup (1400−1500 cm^{-1}).

Measurements revealed a single band, located at 1461 and 1452/1458 cm^{-1} for hexanoate and dodecanoate, respectively (Figure 15a,b, Table 3), which are typical representatives of intermediate and long-chain carboxylates. Compared to the corresponding band of adsorbed propionate, a shift toward higher energies is observed, and the frequency is more similar to CD_3-CH_2COONa. This indicates an extent of coupling of local νCO/νCC and δCH_2 modes similar to acetate and propionate. Obviously, in the hexanoate and dodecanoate ion the terminal CH_3 group is too remote for a significant contribution to the headgroup mode. Notably, there is also no evidence for a CH_3 deformation mode. Although the monolayer/water interfaces of these compounds are known to be rather rough,[22] peaks corresponding to the CH_3 symmetric and antisymmetric mode could be found in the 2800−3000 cm^{-1} region, and thus the orientational average of the molecular hyperpolarizability tensor should be nonvanishing also for a deformation mode. However, it was already concluded from the intensity of the δCH_3 band

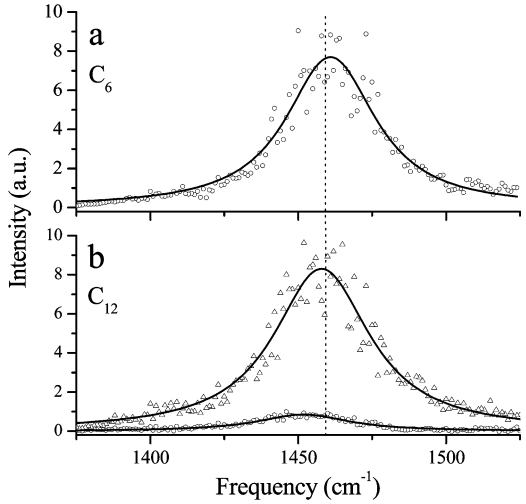

Figure 15. VSF spectra of the sodium hexanoate (aq) and sodium dodecanoate (aq)/CaF_2 interface (a) 46 mM $C_5H_{11}COONa$, (b) 5 (incomplete coverage), 13 μM $C_{11}H_{23}COONa$. Solid lines are fits.

TABLE 3: Fit Parameters of Sodium Hexanoate (aq) and Sodium Dodecanoate (aq) Derived from VSF Spectra at the Liquid/CaF_2 Interface (*ssp* Polarization)

c	ν^a	Γ^a	mode
	$C_5H_{11}COONa$ (aq)/CaF_2		
46 mM	1461	17.4	ν_a
	$C_{11}H_{23}COONa$ (aq)/CaF_2		
5 μM[b]	1452	17.9	ν_a
13 μM	1458	19.0	ν_a

[a] In cm^{-1}. [b] Incomplete coverage.

in methylene-deuterated propionate ion that this band may be greatly enhanced by resonance with the headgroup mode in the case of nondeuterated propionate. Such an energy transfer is not possible between the carboxylate group and the distant terminal CH_3 in any long-chain homologue.

Another interesting feature is the coverage-dependent frequency shift of the headgroup band for dodecanoate (6 cm^{-1}, Table 3). This presumably arises from intermolecular interactions with increasing coverage,[34] which is expected to be stronger for the better aligned adsorbate layers of long-chain carboxylates. Note that even for dodecanoate, the surface adsorption remains a fully reversible process (i.e., all adsorbate-related bands vanished when water was substituted for the sample solution in contact with the fluorite prism). Additionally, the concentrations were far below the critical micellar concentration for dodecanoate.[54] Therefore, the observed shifts cannot be caused by surface-precipitated surfactant aggregates, but arise from a monomolecular layer.

5. Conclusions

This investigation presents the first VSF spectra of the carboxylate headgroup of various aliphatic carboxylates at the liquid/solid interface. The carboxylate bands are located in close proximity to CH deformation bands and could be identified by isotopic substitution. From experiment and calculation, it is now apparent that the simplifying concept of group modes is not generally applicable here because of significant contributions of various group motions to the fundamentals. For some bands, which are prominent in the IR spectrum but SF inactive, combination bands were used to gain further insights. The importance of intensity enhancement, often by Fermi resonance, was also demonstrated.

Furthermore, a number of conflicting assignments reported for adsorbed carboxylates (mainly under UHV conditions) in the CH_2/CH_3 stretch region (2700−3100 cm^{-1}) were resolved using deuterated compounds and selection rules for polarization-dependent VSF spectra. Naturally, accurate assignments are essential for any further analysis of VSF spectra in terms of orientational distributions of organic adsorbates at interfaces.

Adsorption onto fluorite results in significant spectral shifts, caused by the high electrical field at the interface. These effects were particularly strong for headgroup bands. However, the internal modes of vibration of the carboxylate molecules retain their essential character. The reversibility of the adsorption indicates that all studied compounds are linked to the substrate by ionic interactions (i.e., no permanent chemical bonds are formed between the adsorbate and the fluorite crystal). From this perspective, strong effects of pH and ionic strength on the adsorption equilibria can be inferred. A more detailed assessment of this is forthcoming in another paper.[55]

An intensity analysis of the two main bands arising from the orientation of water dipoles at the interface revealed that the effect of the positively charged solid surface extends well into the liquid phase, even at relatively high carboxylate concentrations. With a decreasing number of oriented water molecules, the more well-ordered interfacial states are diminished first. Long-chain surfactant-like carboxylates have a higher affinity to the interface and form layers that more effectively shield the fluorite surface.

Intermolecular interactions of adsorbed carboxylate headgroups are rather small, as evidenced by the almost negligible shift of the corresponding bands. Only for dodecanoate are somewhat larger effects observed.

Using surface selection rules, we were able to ascertain notable differences of VSF studies at the solid/liquid interface compared to measurements performed under UHV conditions. In particular, we observed an inequality in oxygen sites for formate molecules that are tipped.

Acknowledgment. We gratefully acknowledge the financial support of the Department of Energy, Basic Energy Sciences, DEFG02-96ER45557. S.S. appreciates a scholarship of the German Research Foundation (DFG, Bonn), SCHR 1153/1-1. The authors thank D. Beaman and C. McFearin for their invaluable help with the experimental setup.

References and Notes

(1) Davis, J. A.; Hayes, K. F. *Geochemical Processes at Mineral Surfaces*; American Chemical Society: Washington, DC,1986.
(2) Vaughan, D. J.; Pattrick, R. A. D. *Mineral Surfaces*; Chapman & Hall: London, 1995.
(3) Brady, P. V. *Physics and Chemistry of Mineral Surfaces*; CRC Press: Boca Raton, FL, 1996.
(4) Graustein, W. C. K.; Cromack, J.; Sollins, P. *Science* **1977**, *198*, 1252.
(5) Strobel, B. W. *Geoderma* **2001**, *99*, 169.
(6) Nikolić, I.; Blečić, D.; Blagojević, N.; Radmilović, V.; Kovačević, K. *J. Cryst. Growth* **2003**, *252*, 360.
(7) Jiang, B.; Yin, H.; Jiang, T.; Yan, J.; Fan, Z.; Li, C.; Wu, J.; Wada, Y. *Mater. Chem. Phys.* **2005**, *92*, 595.
(8) Ojamäe, L.; Aulin, C.; Pedersen, H.; Käll, P.-O. *J. Colloid Interface Sci.* **2006**, *296*, 71.
(9) Hagfeldt, A.; Grätzel, M. *Acc. Chem. Res.* **2000**, *33*, 269.
(10) Dobson, K. D.; McQuillan, A. J. *Spectrochim. Acta, Part A* **1999**, *55*, 1395.
(11) McQuillan, A. J. *Adv. Mater.* **2001**, *13*, 1034.
(12) Yoon, T. H.; Johnson, S. B.; Musgrave, C. B.; Brown, G. E. J. *Geochim. Cosmochim. Acta* **2004**, *68*, 4505.
(13) Johnson, C. M.; Tyrode, E.; Baldelli, S.; Rutland, M. W.; Leygraf, C. *J. Phys. Chem. B* **2005**, *109*, 321.
(14) Spinner, E.; Yang, P.; Wong, P. T. T.; Mantsch, H. *Aust. J. Chem.* **1986**, *39*, 475.

(15) Kakihana, M.; Kotaka, M.; Okamoto, M. *J. Phys. Chem.* **1982**, *86*, 4385.
(16) Kakihana, M.; Akiyama, M. *J. Phys. Chem.* **1987**, *91*, 4701.
(17) Becraft, K. A.; Richmond, G. L. *Langmuir* **2001**, *17*, 7721.
(18) Shen, Y. R. *The Principles of Nonlinear Optics*; Wiley: New York, 1984.
(19) Richmond, G. L. *Chem. Rev.* **2002**, *102*, 2693.
(20) Superfine, R.; Guyot-Sionnest, P.; Hunt, J.; Kao, C. T.; Shen, Y. R. *Surf. Sci.* **1988**, *200*, L445.
(21) Hore, D.; Beaman, D.; Parks, D.; Richmond, G. *J. Phys. Chem. B* **2005**, *109*, 16846.
(22) Becraft, K. A.; Richmond, G. L. *J. Phys. Chem. B* **2005**, *109*, 5108.
(23) Frisch, M. J.; Trucks, G. W.; Schlegel, H. B.; Scuseria, G. E.; Robb, M. A.; Cheeseman, J. R.; Montgomery, J. A., Jr.; Vreven, T.; Kudin, K. N.; Burant, J. C.; Millam, J. M.; Iyengar, S. S.; Tomasi, J.; Barone, V.; Mennucci, B.; Cossi, M.; Scalmani, G.; Rega, N.; Petersson, G. A.; Nakatsuji, H.; Hada, M.; Ehara, M.; Toyota, K.; Fukuda, R.; Hasegawa, J.; Ishida, M.; Nakajima, T.; Honda, Y.; Kitao, O.; Nakai, H.; Klene, M.; Li, X.; Knox, J. E.; Hratchian, H. P.; Cross, J. B.; Adamo, C.; Jaramillo, J.; Gomperts, R.; Stratmann, R. E.; Yazyev, O.; Austin, A. J.; Cammi, R.; Pomelli, C.; Ochterski, J. W.; Ayala, P. Y.; Morokuma, K.; Voth, G. A.; Salvador, P.; Dannenberg, J. J.; Zakrzewski, V. G.; Dapprich, S.; Daniels, A. D.; Strain, M. C.; Farkas, O.; Malick, D. K.; Rabuck, A. D.; Raghavachari, K.; Foresman, J. B.; Ortiz, J. V.; Cui, Q.; Baboul, A. G.; Clifford, S.; Cioslowski, J.; Stefanov, B. B.; Liu, G.; Liashenko, A.; Piskorz, P.; Komaromi, I.; Martin, R. L.; Fox, D. J.; Keith, T.; Al-Laham, M. A.; Peng, C. Y.; Nanayakkara, A.; Challacombe, M.; Gill, P. M. W.; Johnson, B.; Chen, W.; Wong, M. W.; Gonzalez, C.; Pople, J. A. *Gaussian 03*, revision B.04; Gaussian, Inc.: Pittsburgh, PA, 2003.
(24) Foresman, J. B.; Frisch, Æ. *Exploring Chemistry with Electronic Structure Methods*, 2nd Ed.; Gaussian, Inc.: Pittsburgh, PA, 1996.
(25) Löbau, J.; Wolfrum, K. *J. Opt. Soc. Am. B* **1997**, *14*, 2505.
(26) Miller, J. D.; Hiskey, J. B. *J. Colloid Interface Sci.* **1972**, *41*, 567.
(27) Miller, J. D.; Fa, K.; Calara, J. V.; Paruchuri, V. K. *Colloids Surf., A* **2004**, *238*, 91.
(28) Ishida, H.; Iwatsu, K.; Kubota, J.; Wada, A.; Domen, K.; Hirose, C. *Surf. Sci.* **1996**, *366*, L724.
(29) Yuzawa, T.; Shioda, T.; Kubota, J.; Onda, K.; Wada, A.; Domen, K.; Hirose, C. *Surf. Sci.* **1998**, *416*, L1090.
(30) Kusafuka, K.; Noguchi, H.; Onda, K.; Kubota, J.; Domen, K.; Hirose, C.; Wada, A. *Surf. Sci.* **2002**, *313*, 502−503.
(31) Yamamoto, H.; Akamatsu, N.; Wada, A.; Domen, K.; Hirose, C. *J. Electron Spectrosc. Relat. Phenom.* **1993**, *64/65*, 507.
(32) Domen, K.; Yamamoto, H.; Watanabe, N.; Wada, A.; Hirose, C. *Appl. Phys. A* **1995**, *60*, 131.
(33) Yamakata, A.; Kubota, J.; Kondo, J. N.; Domen, K.; Hirose, C. *J. Phys. Chem.* **1996**, *100*, 18177.
(34) Hayden, B. E.; Prince, K.; Woodruff, D. P.; Bradshaw, A. M. *Surf. Sci.* **1983**, *133*, 589.
(35) Haq, S.; Love, J. G.; Sanders, H. E.; King, D. A. *Surf. Sci.* **1995**, *325*, 230.
(36) Ito, M.; Suetaka, W. *J. Phys. Chem.* **1975**, *79*, 1190.
(37) Ito, K.; Bernstein, H. J. *Can. J. Chem.* **1956**, *34*, 170.
(38) Rotzinger, F. P.; Kesselman-Truttmann, J. M.; Hug, S. J.; Shklover, V.; Grätzel, M. *J. Phys. Chem. B* **2004**, *108*, 5004.
(39) Sexton, B. A. *Surf. Sci.* **1979**, *88*, 319.
(40) Fonteyne, R. *Naturwissenschaften* **1943**, *37/38*, 441.
(41) Newman, R. *J. Chem. Phys.* **1952**, *20*, 1663.
(42) Jakob, P. *Phys. Rev. Lett.* **1997**, *79*, 2919.
(43) Schrödle, S.; Moore, F. G.; Richmond, G. L. University of Oregon, Eugene, OR. Unpublished work.
(44) Wang, C.-Y.; Groenzin, H.; Shultz, M. J. *J. Am. Chem. Soc.* **2005**, *127*, 9736.
(45) Jones, L.; McLaren, E. *J. Chem. Phys.* **1954**, *22*, 1796.
(46) Nakamura, K. *Kagaku Zasshi* **1958**, *79*, 1411.
(47) Kakihana, M.; Kotaka, M.; Okamoto, M. *J. Phys. Chem.* **1983**, 87, 2526.
(48) Kang, I. P. S.; Spinner, E. *Aust. J. Chem.* **1986**, *39*, 465.
(49) Gragson, D. E.; Richmond, G. L. *J. Phys. Chem. B* **1998**, *102*, 3847.
(50) Yuzawa, T.; Kubota, J.; Onda, K.; Wada, A.; Domen, K.; Hirose, C. *J. Mol. Struct.* **1997**, *307*, 413−414.
(51) Wolfrum, K.; Laubereau, A. *Chem. Phys. Lett.* **1994**, *228*, 83.
(52) Lu, R.; Gan, W.; Wu, B. H.; Chen, H.; Wang, H. F. *J. Phys. Chem. B* **2004**, *108*, 7297.
(53) Lu, R.; Gan, W.; Wu, B. H.; Zhang, Z.; Guo, Y.; Wang, H. F. *J. Phys. Chem. B* **2005**, *109*, 14118.
(54) Yan, Y.; Xiong, W.; Huang, J.; Li, Z.; Li, X.; Li, N.; Fu, H. *J. Phys. Chem. B* **2005**, *109*, 357.
(55) Schrödle, S.; Moore, F. G.; Richmond, G. L. *J. Phys. Chem. C.*, submitted for publication, 2007.